

Article

# Integration of Different Storage Technologies towards Sustainable Development—A Case Study in a Greek Island

Maria Margarita Bertsiou \*  and Evangelos Baltas

Department of Water Resources and Environmental Engineering, School of Civil Engineering, National Technical University of Athens, 5 Iroon Polytechniou, 157 80 Athens, Greece; baltas@chi.civil.ntua.gr

\* Correspondence: mbertsiou@chi.civil.ntua.gr; Tel.: +30-2107722413

**Abstract:** The necessity for transitioning to renewable energy sources and the intermittent nature of the natural variables lead to the integration of storage units into these projects. In this research paper, wind turbines and solar modules are combined with pumped hydro storage, batteries, and green hydrogen. Energy management strategies are described for five different scenarios of hybrid renewable energy systems, based on single or hybrid storage technologies. The motivation is driven by grid stability issues and the limited access to fresh water in the Greek islands. A RES-based desalination unit is introduced into the hybrid system for access to low-cost fresh water. The comparison of single and hybrid storage methods, the exploitation of seawater for the simultaneous fulfillment of water for domestic and agricultural purposes, and the evaluation of different energy, economic, and environmental indices are the innovative aspects of this research work. The results show that pumped hydro storage systems can cover the energy and water demand at the minimum possible price, 0.215 EUR/kWh and 1.257 EUR/m<sup>3</sup>, while hybrid storage technologies provide better results in the loss of load probability, payback period and CO<sub>2</sub> emissions. For the pumped hydro–hydrogen hybrid storage system, these values are 21.40%, 10.87 years, and 2297 tn/year, respectively.

**Keywords:** energy transition; storage technologies; pumped hydro storage; batteries; fuel cell; desalination; sustainable development; energy independence; water independence; water resources management



**Citation:** Bertsiou, M.M.; Baltas, E. Integration of Different Storage Technologies towards Sustainable Development—A Case Study in a Greek Island. *Wind* **2024**, *4*, 68–89. <https://doi.org/10.3390/wind4010004>

Academic Editor: Javier Serrano González

Received: 22 September 2023

Revised: 3 February 2024

Accepted: 22 February 2024

Published: 1 March 2024



**Copyright:** © 2024 by the authors. Licensee MDPI, Basel, Switzerland. This article is an open access article distributed under the terms and conditions of the Creative Commons Attribution (CC BY) license (<https://creativecommons.org/licenses/by/4.0/>).

## 1. Introduction

Climate change provides proof of the urgent need for the transition to Renewable Energy Sources (RES) [1]. By 2020, the EU had achieved a 31% reduction in greenhouse gas emissions, exceeding its objective for a 21.3% share of RESs in the final energy consumption and improved energy efficiency by 17.5%, according to EEA [2]. The framework for keeping global warming below 2 °C, according to pre-industrial levels, and to pursue efforts to reduce the temperature increase to 1.5 °C is outlined in the Paris Agreement on Climate Change [3]. The Paris Agreement is the culmination of years of negotiations and efforts by the international community to address the issue of climate change. Enhancing countries' ability to adapt to climate change, boosting ecosystems' resilience, and facilitating the transition to low-carbon economies are the main goals of the Paris Agreement. Greece, as a member of the EU, tries to increase the proportion of RESs in the energy balance.

Reducing greenhouse gas emissions is one of the main advantages of the transition to RES [4,5]. Large volumes of carbon dioxide are released by fossil fuels including oil, coal, and gas, which worsen the environment and human health in addition to their penetration of climate change [6]. These emissions are decreased, and the harmful effects of climate change are controlled by the use of RES. By depending on local, sustainable power sources, RESs have an important role in the reduction in energy costs [7] and the enhancement of energy security [8,9]. Finally, transitioning to RESs can also create jobs and boost economic growth [10]. Over 11 million people worldwide were employed in the renewable energy sector in 2018, according to the International Renewable Energy Agency

(IRENA). This number is expected to continue growing as countries invest in renewable energy infrastructure and technologies.

Besides the benefits of renewable energy sources, there are also significant challenges that come with the transition. One of the main challenges is technical and operational problems [11] from adapting infrastructure to accommodate new sources of power. Many power grids are designed to handle large, centralized power plants, making it difficult to integrate smaller, decentralized sources of renewable energy [12], leading to issues in stability and power quality. Another challenge is the intermittent nature of renewable energy sources [13], particularly solar and wind power sources. Unlike traditional power plants that can generate a consistent amount of energy, RESs rely on weather conditions to generate power. This intermittent behavior makes it challenging to predict and manage energy supply, requiring new approaches to energy management and storage [14,15]. Also, excess energy from wind and solar systems can contribute significantly to better water and energy management with the integration of a storage system [16]. Finally, transitioning to RESs will require significant government, financial, and social support [17]. Many countries and industries still heavily rely on fossil fuels, and the transition to RES will require significant policy changes, investment, and public support [18].

A significant impact on the energy supply, due to the COVID-19 pandemic, has been observed. This impact occurred due to the production, transportation, and storage difficulties of produced energy [19]. Due to the decline in energy consumption, the oversupply of energy led to a reduction in the investment of such projects. The COVID-19 pandemic is a key factor in the energy transition, while during the pandemic concerns were raised about how crisis-resilient energy systems react to such crises [20], and the necessity for flexible and diverse energy sources and systems was underlined.

On the other hand, water availability is affected by climate change since the latter is interlinked with the water cycle [21]. Climate factors that affect the main sector of agriculture are predicted to deteriorate, according to forecasts [22]. The length of the growing season is anticipated to shorten, which will affect agricultural production in general. The interdependence of water, energy, and food to the attainment of a stable society and economic development is highlighted by the Water–Energy–Food Index (WEF) [23]. Although food and water are the two essentials for survival, energy is also necessary to support residential, industrial, and transportation operations in a society, as well as to guarantee the production of food and water [24]. However, the capability to produce power to meet energy demands may be impacted by the accessibility to water resources [25].

The average cost of transporting fresh water to the islands from the mainland, in Greece, is currently around 8.2 €/m<sup>3</sup> [26]. Additionally, the use of Local Power Stations (LPS) that provide the required amounts of energy results for expensive power production, blackouts during the peak tourist season, reliance on fossil fuels, and inconsistent network operation. A solution to the energy and water problems would be Hybrid Renewable Energy Systems (HRES), which combine one or more RES and one or more storage technologies. The problems caused by the stochastic nature of natural variables, particularly wind speed and solar irradiation, can be resolved by this integration [27]. Also, such a solution can contribute to RES integration, improve the WEF nexus, increase network reliability and performance, and lead to a reduction in CO<sub>2</sub> emissions. The issue of inadequate domestic and irrigation water is also resolved by integrating a desalination unit (DU) into the HRES and by desalinating the seawater surrounding the islands.

## 2. State of the Art

Previous research has been conducted on the integration of RES units with storage units. In [28], an economic analysis of an HRES shows that an HRES consisting of photovoltaic modules (PV), diesel generators (DG) and batteries (BT) in an island in Qingdao, China, reduces around 0.14 EUR/kWh of the cost of energy and saves up to 236 tn/year, compared to a system without energy storage. The optimal size of an HRES, in [29], consisting of WT, PV, BT and flywheel storage, is achieved through a multi-objective optimization

approach for meeting the load demand in remote areas in Kenya. The results show that adopting an energy storage system can lead to an annual gain potential of 858 kWh. An optimization method using genetic algorithm (NSGA)-II and HOMER Pro (3.14) software, in [30], for an HRES in Kutubdia Island in Bangladesh, investigates how a reduction in the net present cost (NPC), cost of energy (COE), and CO<sub>2</sub> emissions of the proposed power system can be achieved. The results show that a PV/WT/BT/DG system has the lower NPC, while NPC obtained by the NSGA-II algorithm is 2.69% lower than that based on HOMER. In [31] a techno-economic-environmental analysis using multi-objective optimization is performed for different scenarios of HRES consisting of different combinations of WT/PV/Pumped Hydro Storage (PHS)/BT/DG. A pumped battery hybrid storage scenario is also examined. The results show that the emissions of the proposed systems range from 0.072 to 0.148 kg/kWh of served load and configurations, based on PHS, receive the highest ratings, among all of the other options. In [32] an evaluation of a WT/PV/Fuel Cell (FC) system is conducted. The levelized cost of energy (LCOE) is around 0.210 EUR/kWh for on-grid systems and about 0.390 EUR/kWh for off-grid systems. He et al. [33] conducted a techno-economic analysis for the comparison of HRES consisting of WT and PV and different energy storage systems, i.e., BT, PHS, Hydrogen and Thermal Energy Storage (TES), using a multi-objective capacity optimization. Results about the LCOE demonstrate that TES is the most economical option.

The integration of a desalination unit with an HRES has also acquired great interest in recent years. The economic viability of desalination plants powered by RES is investigated in [34]. The results show that the projects can be economically profitable under certain conditions of grants and the investors' expected benefits, but sales of water and energy can be limiting factors. In [35], a hybrid optimization algorithm is used for a PV/WT/DG/BT HRES, which supplies energy and water to a non-connected island in Bangladesh, resulting in the COE of the optimum system at 0.220 EUR/kWh. In [36], a cost-benefit analysis has been conducted for an HRES consisting of WT/PHS for the fulfillment of electricity and water demand in an anhydrous island. The environmental impacts of three optimized HRES for the desalination of seawater are accessed in [37], showing that produced freshwater by a WT/BT system had less impact on resources, climate, and ecosystem quality compared to a PV/BT or a WT/PV/BT system. In [38], an analysis based on energy, economic, and environmental factors between two HRES of different storage technologies, i.e., PHS and BT, and consisting of both WT/PV is conducted. Results show that the integration with a battery has a higher LCOE and payback period (PBP), while less use of costly and polluting conventional fuels is achieved.

After a thorough review, a few studies investigate how the integration of different energy storage technologies affects the final performance of an HRES, in terms of the fulfillment of the energy demand and the price of the produced energy. Also, a few studies examine the differences between simple and hybrid storage, i.e., the use of more than one storage technology. The comparison of different methods of storage, i.e., PHS, BT, and FC, as well as two alternative combinations of them (hybrid storage), i.e., pumped hydro-battery hybrid storage (PHBH) and pumped hydro-hydrogen hybrid storage (PHFC) for the simultaneous fulfillment of energy and water requirements is one of the innovative aspects of this research work in the context of HRES. The integration of a desalination unit, for covering water needs in an HRES combined with hybrid storage technologies as presented in this paper, has not been investigated yet. With the integration of a DU, this research study investigates the capability of energy supply for both household electricity and energy requirement for water for domestic and agricultural purposes, by simultaneously comparing different storage technologies. For water requirements, data from the crops are obtained to include both water demand for domestic and agricultural purposes, filling, also, the gap in the fulfillment of agricultural water in areas that suffer from water scarcity. This research paper tries to answer which storage solution, in combination with wind turbines, photovoltaic modules, and desalination units, leads to the coverage of most energy and water demands with the lowest possible environmental cost and the best final

offer price. The analysis of the environmental cost includes the reduced use of fossil fuels and, consequently, the reduction in greenhouse emissions. At the end of this research, a sensitivity analysis shows how changes in meteorological, demographical, and installation factors affect the results. The idea behind this approach is to provide the capability to the “decision maker”, that means the local community, the ministry, or the manufacturer, to choose the storage technology that best fits their specific area (wind/solar potential, topography) and their specific demands (household consumption, domestic and irrigation water, tourism increase). In this regard, a process-based model is developed to investigate the final cost of water, cost of energy, loss of load probability, payback period, and reduced emissions, along with the penalty from the Emissions Trading System for five HRESs using different storage technology (single or hybrid), in a Greek island, which suffers from water scarcity and energy, blackouts, and dependence on conventional fuels.

### 3. Materials and Methods

#### 3.1. Study Area

The study area is a non-interconnected island in the North Aegean Sea, Fourni Korseon. The main inhabited areas are Fourni, Thymena, and Agios Minas. Fourni is the largest island of the cluster, and it is the capital settlement with the same name. Additionally, Chrysomilia, with fewer than 100 inhabitants, has been connected to a water supply network and to a desalination plant with a capacity of 100 m<sup>3</sup>/day since 2008. However, the main village, Fourni, in the center of the island with 1400 inhabitants and the largest tourist traffic, does not have a desalination unit, and today the supply of fresh water is delivered from a tap, leading to an extensive use of bottled water. To meet its energy needs, the island has an undersea connection to the neighboring island of Samos, causing lengthy blackouts. During periods of increased energy demand, especially in the summer months due to tourism, the problem is exacerbated. Although the island has both great wind and solar potential, neither resource has yet been fully utilized.

#### 3.2. Demand and Meteorological Data

Domestic water requirements have been estimated according to the monthly population, while water for agricultural use has been estimated based on the crops of the island and the calculation of the evapotranspiration [39] for these areas during irrigation season, April to September. The desalination of seawater is supposed to be performed by the reverse osmosis (RO) method. The estimated energy consumption for RO is 5.85 kWh/m<sup>3</sup> [40,41]. Monthly data about electric load are provided by the Public Power Corporation of Greece, and their aggregation into an hourly step is based on the consumption profile for Athens by Psiloglou et al. [42].

Data about the wind potential, temperature, and precipitation are obtained from the National Observatory of Athens Automatic Network-NOANN [43], and specifically from the weather station that is installed on the island. It must be noted that data about solar irradiance are obtained from the weather station of Samos Island, as in the station of Fourni there are no measurements of solar irradiance. For the calculation of the energy from the PV, the irradiance on the tilted plane is used, where the tilted plane is the inclination of the PV frame. This angle must be optimal for every month in order to make the best use of the solar potential and the PVs for energy production. To find the optimal angle for the study area, the radiation is calculated for each month on the tilted plane, and each month the PV is considered to have the optimal angle. In Table 1, the monthly energy requirements for the desalination of water for domestic and agricultural use as well as the energy requirements for household consumption (electric load) are presented.

**Table 1.** Monthly electricity requirements for desalination and household consumption.

Month	Domestic Water (kWh)	Irrigation Water (kWh)	Household Consumption (kWh)	Total Consumption (kWh)
1	31,590	-	665,446	697,036
2	31,590	-	601,048	632,638
3	31,590	-	665,446	697,036
4	31,590	5778	495,990	533,358
5	42,120	117,192	296,050	455,362
6	59,670	151,177	286,500	497,347
7	70,200	170,315	434,000	674,515
8	91,260	153,850	504,835	749,945
9	42,120	60,788	162,840	265,748
10	31,590	-	168,268	199,858
11	31,590	-	325,680	357,270
12	31,590	-	665,446	697,036
TOTAL	526,500	659,100	5,271,549	6,457,149

### 3.3. Modeling of Resource Components

The estimation of the produced energy from a wind turbine is based on its power curve provided by the manufacturer. The power curve shows the correlation between the power output of the WT and the wind speed at hub height, considering the power coefficient. Enercon E-44's 900 Kw power curve is employed in this study. Wind speed data are obtained at the altitude where the weather station is installed. To determine the wind speed at the hub height of the wind turbine, an equation is used for the representation of the height dependence of the wind speed, which is based on the roughness height parameter of the installation surface [44].

PVs compared to other RESs are superior due to their ability for direct electricity production, their silent mode operation, and the fact that they can be gradually implemented into an RES system. Also, they produce zero CO<sub>2</sub> emissions, they require minimum maintenance costs, they have a long lifetime, and their installation is more aesthetically acceptable compared to other RESs and especially to WTs. To estimate the output of a PV,  $P_{PV}(t)$ , Formulas (1)–(3) have been used [45]:

$$P_{PV}(t) = P_{STC} \cdot \frac{G_t(t)}{G_{STC}} \cdot PR_{PV} \cdot PR_{inv} \cdot PR_{grid} \cdot PR_T(t), \quad (1)$$

$$PR_T(t) = 1 - \gamma \cdot [T_C(t) - T_{C,STC}], \quad (2)$$

$$T_C(t) = T_{amb}(t) + (NOCT - T_{NOCT}) \cdot \frac{G_t(t)}{G_{NOCT}}, \quad (3)$$

where  $P_{STC}$  is the the peak capacity of the PV array (W/m<sup>2</sup>),  $G_t(t)$  is the global solar irradiance on the inclined surface (W/m<sup>2</sup>),  $G_{STC}$  is the standard radiation parameter and is equal to 1000 W/m<sup>2</sup>,  $PR_{PV}$  is the efficiency of a PV system (%),  $PR_{inv}$  is inverter efficiency (%),  $PR_{grid}$  is the grid-connected efficiency (%),  $PR_T(t)$  is the efficiency parameter related to the temperature of the PV cell (%),  $\gamma$  is the PV module efficiency temperature coefficient (/°C),  $T_C(t)$  is the temperature of PV cells (°C),  $T_{C,STC}$  is the reference standard temperature of PV modules, equal to 25 °C,  $T_{amb}(t)$  is the ambient temperature (°C),  $NOCT$  refers to the operating temperature of PV modules under the ambient temperature of  $T_{NOCT}$ , equal to 20 °C, and under the environment of solar irradiance  $G_{NOCT}$ , equal to 800 W/m<sup>2</sup>.

It is assumed that twin-shift tracking stents are coupled with the series-parallel-connected PVs, helping in the rotation of the PVs and ensuring the perpendicular incidence of the solar irradiance. In this way, the utilization of the maximum solar energy is achieved [46]. The conversion of direct current, produced by the PV, to alternative current (AC), is performed through the connection with an inverter. PVs produce most of their energy at the point where there is the intersection of the load with the current voltage,

according to the voltage–current curve (I–V) of the PV. In real-time operations, the load mismatch and the variation in the solar irradiance and the temperature prevent this intersection [47]. To surmount this and to consistently maximize the PVs' output in accordance with the temperature and the solar irradiation, it is assumed that PVs are connected to the inverter through the Maximum Power Point Tracking control (MPPT) [48]. This means that the produced power output of the PVs is supposed to be at every time-step equal to the maximum power [49].

In order to accommodate the intermittent nature of both renewable energy sources, storage technology must be used to meet the supply and demand, simultaneously. PHS, BT, FC, PHBH and PHFC are employed as storage systems in this research study.

The storage units exploit the surplus energy,  $E_{sur}$  (kWh), from the WTs and the PVs. The PHS uses this energy to pump seawater to a reservoir at a high altitude, through the pumping station. The release of water from the reservoir at a higher altitude when the demand for electricity is higher, in order to flow toward the reservoir at the lower altitude, generates electricity for the island's electricity grid through the hydroelectric plant. The reservoir's altitude and the available water both affect how much energy is produced. The stored water in the higher reservoir from time step  $t-1$  is added to the water from the next time step. The benefit of this procedure is the potential to store surplus energy and exploit it when the demand is high or when the RES potential is low, even though more energy is needed for pumping water than is generated through the hydro turbine. The volume of the pumped water  $V_p$  (m<sup>3</sup>) and the produced hydro energy,  $E_{def}$  (kWh), for every time step, are given by Formulas (4) and (5) [50]:

$$V_p = \frac{E_{sur} \cdot PR_p}{\rho \cdot g \cdot H}, \quad (4)$$

$$E_{def} = \rho \cdot g \cdot H \cdot V_h \cdot PR_t, \quad (5)$$

where  $PR_p$  is the pumping efficiency (%),  $\rho$  is the density of the water (kg/m<sup>3</sup>),  $g$  is the acceleration due to gravity (m/s<sup>2</sup>) and  $H$  is the net head (m).  $V_h$  is the amount of released water from the upper reservoir (m<sup>3</sup>) and  $PR_t$  is the turbine efficiency (%). In the simulations, it is assumed, for safety reasons, that the reservoir's lower limit cannot be less than 10% of its total capacity. The pumped hydro storage system consists of the upper reservoir, the pumping station, and the hydro turbine.

The charging of the battery, in the case of surplus energy, is estimated by Formula (6), while its discharge is estimated using Formula (7):

$$SOC(t) = SOC(t-1) \cdot (1 - \sigma) + E_{sur} \cdot PR_{bat}, \quad (6)$$

$$SOC(t) = SOC(t-1) \cdot (1 - \sigma) - E_{def} \cdot PR_{bat} \quad (7)$$

where  $SOC(t)$  is the state of charge at time  $t$  (kWh),  $SOC(t-1)$  is the state of charge at time  $t-1$  (kWh),  $\sigma$  is the self-discharge rate (%) and  $PR_{bat}$  is the efficiency of the battery (%). Self-discharge rate describes a battery's decreasing level of charge when it is not in use. The new SOC for each time step depends not only on the efficiency of the battery and the energy surplus or deficit, but also on the state of charge of the previous time step, which is always affected by the self-discharge rate, even if the battery is on standby. Also, it is assumed that the minimum state of charge of the battery cannot be less than  $(1 - DOD)$  the total capacity of the battery, due to safety reasons, where  $DOD$  is the depth of discharge of the battery (%) and is given by the manufacturer.

Hydrogen can be produced using an electrolyzer, which converts surplus energy to hydrogen through the electrolysis. Electrolysis requires desalinated water. The hydrogen produced by the surplus energy is estimated using Formula (8), while the produced energy from the fuel cell is estimated using Formula (9) [51]:

$$H_2 = E_{sur} \cdot PR_{el} / 37.8 \quad (8)$$

$$E_{FC} = H_2 \cdot PR_{FC} \cdot 37.8 \quad (9)$$

where  $PR_{el}$  is the efficiency of the electrolyzer (%) and  $PR_{FC}$  is the efficiency of the fuel cell (%).

When there is surplus energy, the amount of hydrogen remaining in the hydrogen tank at the time step  $t$ ,  $H_2^{tank}(t)$ , is estimated by (10), while, when there is an energy deficit it is estimated according to Formula (11):

$$H_2^{tank}(t) = H_2^{tank}(t-1) + H_2(t) \quad (10)$$

$$H_2^{tank}(t) = H_2^{tank}(t-1) - H_2(t) \quad (11)$$

It is assumed that the lower limit of the hydrogen tank cannot be less than 10% of the total capacity due to safety reasons.

The assumptions for the technical characteristics of all storage technologies are presented in Table 2.

**Table 2.** Technical characteristics of storage technologies.

Parameter	Value
Net head (m)	192
Days of autonomy	2
Pumping station efficiency (%)	78
Hydro turbine efficiency (%)	90
Battery efficiency (%)	82
Inverter efficiency (%)	82
Depth of discharge, DOD (%)	80
Self-discharge, $\sigma$ (%)	2
Electrolyzer efficiency (%)	90
Fuel cell efficiency (%)	50

A desalination unit is coupled in all scenarios for the fulfillment of required water for domestic and agricultural purposes, using water from the sea. Also, the desalination unit is necessary in scenarios where energy is stored through the production of hydrogen. In these cases, the generation of green hydrogen presupposes the electrolysis of pure desalinated water.

### 3.4. Configurations and Energy Management Strategy

In this section, the configurations that will be examined, based on the combination of the RES and the storage methods that were analyzed in the previous section, are presented. A storage system is coupled in all configurations as the stochastic nature of the RES (wind and solar) potential prevents the simultaneous satisfaction of demand in correspondence with renewable energy production. Based on the configuration examined, a PHS, a BT, and an HT are used for the storage of excess energy. Also, two configurations with hybrid storage technologies are evaluated; a pumped hydro–battery hybrid storage (PHBH), which consists of a PHS and a battery, and a pumped hydro–hydrogen hybrid storage (PHFC), which consists of a PHS, an electrolyzer, and a fuel cell. Also, in all of the configurations a desalination unit is coupled for the satisfaction of domestic and irrigation water supply.

The three RES (wind, solar, and hydro) and the performance of various storage systems (PHS, battery, hydrogen) form the foundations for the suggested energy management scenarios for both single and hybrid storage. These scenarios compare the effectiveness of these storage methods in meeting basic needs of society, i.e., electricity and fresh water. In the first configuration (WT/PV/DU/PHS), the PHS is used for the exploitation of the surplus energy. In Configuration 2 (WT/PV/DU/BT), the storage method involves the use of batteries, instead of the PHS system of Configuration 1. In the third configuration (WT/PV/DU/FC), the battery has been replaced with a hydrogen production and utilization system. In Configuration 4 (WT/PV/DU/PHBH), a hybrid pumped battery storage system, consisting of a PHS and a battery, is used, and in the fifth configuration

(WT/PV/DU/ PHFC) the hybrid storage system consists of a PHS, an electrolyzer, and a fuel cell. In Table 3, the configurations that are examined in this study are presented.

**Table 3.** Configurations of HRES examined.

Configuration	1	2	3	4	5
WT	✓	✓	✓	✓	✓
PV	✓	✓	✓	✓	✓
DU	✓	✓	✓	✓	✓
PHS	✓			✓	✓
BT		✓		✓	
FC			✓		✓

The nominal capacities of the installed WTs and PVs are selected based on the meteorological data (wind and solar potential, temperature, precipitation), on the island's requirements for energy and freshwater (household consumption, domestic and irrigation water), and according to the methodology described in [52]. The HRES's number of autonomous days is used to dimension the storage systems (reservoir [52], batteries [53], hydrogen tank [54]). This number provides the days that the storage unit of the HRES provides the required energy for the demands of the island, even if the RES potential is low and no energy can be produced by the WTs and the PVs. Energy storage systems typically consider two days of autonomy [55]. Additionally, it is assumed that the hydrogen tank and batteries will be at their lowest capacities at the beginning of the simulation and that the reservoir will be 50% filled. By using the extra energy generated by WTs and PVs, seawater is pumped into the higher reservoir. It must be noted that this reservoir does not provide water to the desalination unit of the island. The DU is supplied with seawater and adds fresh water to the desalination reservoir. The pumps need a surplus of energy to function properly, and if there is not sufficient energy for them to start their operation, then no water is pumped to the upper reservoir. The pumping station must be capable of absorbing the maximum RES output minus the energy that is given to fulfill the demands, and its nominal power is calculated using [52]. The same applies to determining the hydro turbine's rated power. It must be ensured that in the case of low wind potential, it can handle the maximum load [52]. For the sizing of the fuel cell and the electrolyzer, it is considered that the first is capable of handling any electrical demand that cannot be met by other RES or storage systems, according to [54], depending on the configuration under examination, and the second can convert any surplus energy into hydrogen at each time step [54]. Data of the installed components of each configuration is presented in Table 4. Depending on the scenario under consideration, load demand not met by WTs, PVs, PHS, BT, or FC is met by the grid, which necessitates the startup of the nearby power plant. To control the response of the HRES and its reliability in covering the required demand for electricity and drinking and irrigation water supply, the simulations are performed with hourly data inputs, to guarantee the highest possible reliability of the results.

**Table 4.** Data of the installed components of each configuration.

Configuration	PHS	BT	FC	PHBH	PHFC
WT (MW)	1.8	1.8	1.8	1.8	1.8
PV (MW)	2.0	2.0	2.0	2.0	2.0
DU (m <sup>3</sup> /day)	1309	1200	1320	1300	1300
Upper reservoir (m <sup>3</sup> )	75,243	-	-	37,621	37,621
Pumps (kW)	2.6	-	-	1.25	1.25
Hydro turbine (MW)	1.2	-	-	0.85	0.85
Battery (kWh)	-	60,000	-	30,000	-
Electrolyzer (MW)	-	-	2.8	-	2.6
Fuel cell (MW)	-	-	1.9	-	1.9
Hydrogen tank (kg)	-	-	1876	-	938

The first three configurations of the HRESs are considered to have simple storage, i.e., a single storage unit for the surplus energy. The storage strategy followed is shown in Figure 1. The procedure is performed for one year of data ( $i = 8760$ ). Meteorological data and the island's demand statistics are provided as inputs. The WTs and PVs' combined energy output is estimated according to the under-consideration configuration. In every configuration, priority is given to the domestic water, after to the irrigation water and at last to the energy for electricity demand. The renewable energy produced is calculated (RES) for each step and it is determined if the corresponding demand can be met, according to the priority and according to the produced renewable energy. When all demands have been checked it is determined whether there is surplus energy  $E_{sur}$ . If there is excess energy, the available storage space in the storage unit is checked. If there is no space, then, unfortunately, the excess energy is rejected. That means that the produced energy cannot be utilized by the grid or by the storage unit. This happens repeatedly in every installed RES project without the integration of storage technology, where produced RES energy cannot be utilized. An attempt to avoid this is by the incorporation of a storage unit. If there is additional space in the examined storage unit then the storage unit's new state of charge is determined, always ensuring that the maximum state of charge level of the storage unit is not exceeded and the fulfillment of the demands is estimated for this time step. For every time step (hourly time steps) the met and unmet demands are estimated at first according to the produced renewable energy and afterward according to the stored energy to each of the storage units, based on the scenario examined. That means how many kWh of household consumption and how many cubic meters of desalinated domestic and irrigation water can be satisfied at the end of each time step. Also, it is determined whether there is available stored energy in the storage unit if there is no surplus energy,  $E_{sur} < 0$ , but there is still unmet demand. If stored energy is accessible, the new state of charge is determined and finally, the fulfilled and unmet demands for an hour are once more approximated.

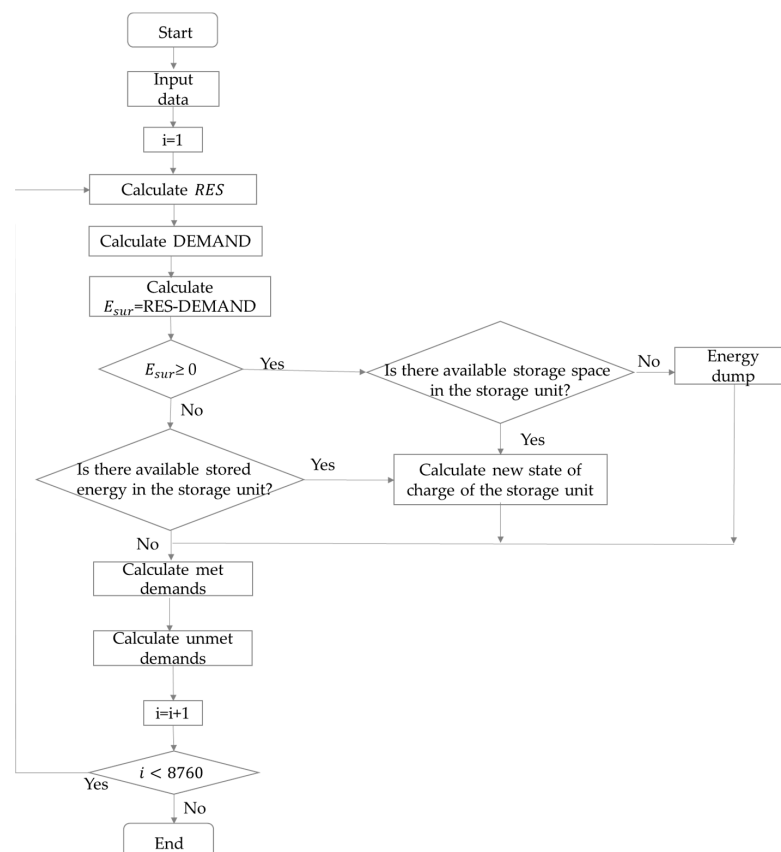


**Figure 1.** Basic energy management strategy for single-storage HRES.

Within the last two configurations, there is hybrid storage, i.e., a combination of two different storage methods. The storage strategy followed is shown in Figure 2. The step is, again, conducted hourly and the procedure is performed for one year of data ( $i = 8760$ ). Again, as in the simple storage method, the data are entered, and the process is no different until the control of excess energy  $E_{sur}$ . After this step, the method of controlling and utilizing the excess energy differs. As it is shown in the flowchart, if there is excess energy, the first storage unit is checked for available storage space. If there is available space, then the new state of charge of the first storage unit is calculated. If not, or if there is still excess energy, the second storage unit is checked for available storage space. If there is available space, then the new state of charge of the second storage unit is calculated. If not, or if there is still excess energy after the charging of the second storage unit until its maximum state of charge level, then unfortunately the excess energy is rejected. In both storage units, it is always checked that the maximum state of charge level is not exceeded when they are in charging mode. If there is no excess energy but there is still demand that has not been fulfilled, the first storage unit is checked for available stored energy. If there is available stored energy, then the new state of charge is calculated. If not, or if there is still unmet demand, the second storage unit is checked for available stored energy. If there is available stored energy, then the new state of charge is calculated and, in any case, it is checked if there is still an unmet demand, and both met and unmet demand is estimated for each step.

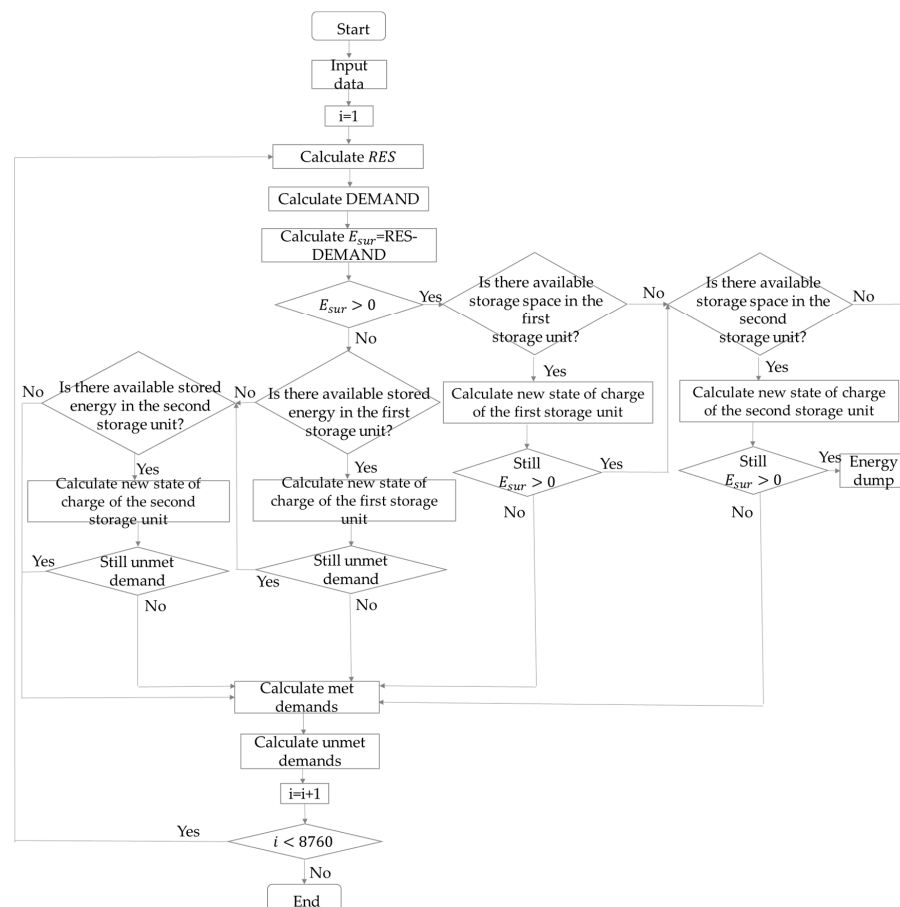


Figure 2. Basic energy management strategy for hybrid storage HRES.

### 3.5. Evaluation Analysis

For the evaluation and the comparison of the different configurations of the HRES indices about energy, economic and environmental analysis are estimated. The loss of load (LOL), the loss of load probability (LOLP), the cost of energy (COE), the cost of

water ( $COW$ ), the payback period ( $PBP$ ) and eliminated amounts of  $CO_2$  ( $EM_{CO_2}$ ) are also estimated.

Formulas (12) and (13) estimates  $LOL$  and  $LOLP$  respectively, for the evaluation of the reliability of each HRES:

$$LOL_j = \sum_{i=1}^{8760} E_j^{loss} \quad (12)$$

$$LOLP_j = \frac{LOL_j}{\sum_{i=1}^{8760} E_j^{load}} \quad (13)$$

where  $j$  indicates the specific demand of energy that is about to be fulfilled or not, between energy for domestic water desalination,  $d$ , energy for irrigation water desalination,  $ir$ , and energy for household consumption,  $h$ . The hourly time steps for one year (1–8760) are indicated by index  $i$ , and  $E_j^{loss}$  is the loss of load of each demand  $j$ .

Formula (14) estimates the  $COE$  [56] as follows:

$$COE = \frac{CAPEX + \sum_{n=1}^N OPEX + C_{rpl} - C_{slv}}{E_{hres}} \quad (14)$$

$$C_{slv} = C_{rpl} \cdot \left\{ \frac{LF_{comp} - \left[ LF_{hres} - \left( LF_{comp} \cdot \text{integer} \left( \frac{LF_{hres}}{LF_{comp}} \right) \right) \right]}{LF_{comp}} \right\} \cdot \left[ \frac{1}{(1+r)^{LF_{hres}}} \right] \quad (15)$$

where  $CAPEX$  is the initial investment cost of the HRES (in EUR),  $OPEX$  is the operating and maintaining costs of each component (in EUR),  $C_{rpl}$  is the cost of replacing the component at the end of its lifetime (in EUR),  $C_{slv}$  is the salvage cost (in EUR),  $n$  is the lifetime of the HRES (1, 2, ...,  $N = 25$ ), and  $E_{hres}$  is the produced energy by the HRES (in kWh). The salvage cost [51] is estimated separately for each component, according to Formula (15), where  $LF_{comp}$  is the lifetime of each component,  $LF_{hres}$  is the lifetime of the HRES, and  $r$  is the discount rate (%). The initial costs represent the initial investment, installation, and replacement costs of the system, including the cost of each unit, depending on the configuration examined. The initial cost does not include any subsidies from the national or local government policies. The operation and maintenance costs refer to the corresponding costs for the total life; 25 years of an HRES.

In order to recover the full cost of the investment, the  $PBP$  determines project's required years of operation. It is based on net annual savings ( $AS$ ) and the overall investment cost. Formula (16) provides a mathematical description of it:

$$PBP = \frac{CAPEX + \sum_{n=1}^N OPEX}{AS} \quad (16)$$

The net annual savings contains the net revenue it is expected to earn each year by using the HRES instead of other energy sources.  $PBP$  is determined using the current kWh pricing and the current cost for desalinated water. According to the PPC, the average tariff, based on different consumptions (daytime or nighttime consumption), determines the cost of a kWh. Today, the price is 0.22833 €. (Public Power Corporation, Athens, Greece, 2023). However, such projects can be more competitive by a reduction in the selling price gap. This can be achieved in the event of an increase in energy prices. Freshwater for the islands costs between 7 and 12 €/m<sup>3</sup> [26,57], and in this study, is considered equal to 10 €/m<sup>3</sup>. It is important to note that the  $PBP$  calculation evaluates the financial viability of a project without considering other factors that may impact the return on investment, such as inflation, tax benefits, or changes in energy prices over time.

Formula (17) is used to calculate the amounts of CO<sub>2</sub> that the HRES system eliminates,  $EM_{CO_2}$  (tn/year), when 1 kWh supplied by the HRES replaces 1 kWh provided by the LPS as follows:

$$EM_{CO_2} = \frac{[E_{PV} \cdot (F_{grid} - F_{PV}) + E_{WT} \cdot (F_{grid} - F_{WT})]}{10^6} \quad (17)$$

where  $E_{WT}$  and  $E_{PV}$  are the generated energy from the WTs and the PVs, respectively.  $F_{WT}$  and  $F_{PV}$  are the emission factors of the WTs and the PVs and are equal to 13.7 g CO<sub>2</sub>/kWh and 50 g CO<sub>2</sub>/kWh, respectively [58].  $F_{grid}$  represents the emission factor of each country's grid. According to the country datasheet, the GHG intensity of electricity production for Greece in 2021 is about 397 g CO<sub>2</sub>/kWh [59]. One ton of CO<sub>2</sub> is priced according to the market rate for a ton on 10 September 2023 [60], which is 81.52 EUR/tn. Note that its price displays an average daily increasing trend of 0.6%. In Table 5, the data used for the economic evaluation are presented.

**Table 5.** Data for the economic evaluation.

Component	Parameter	Value (Unit)
Wind turbine [61]	CAPEX (EUR/kW)	906
	OPEX (EUR/kW)	136
	LF (years)	25
Photovoltaic module [31]	CAPEX (EUR/kW)	800
	OPEX (EUR/kW)	11.2
	LF (years)	25
Desalination unit [51]	CAPEX (EUR/m <sup>3</sup> /day)	484
	OPEX (EUR/m <sup>3</sup> /day)	0.32
Reservoir [33]	CAPEX (EUR/m <sup>3</sup> )	154
	OPEX (EUR/m <sup>3</sup> )	3.1
	LF (years)	35
Hydro turbine [33]	CAPEX (EUR/kW)	910
	OPEX (EUR/kW)	18
	LF (years)	10
Pumping station [33]	CAPEX (EUR/kW)	217
	OPEX (EUR/kW)	4.35
	LF (years)	20
Battery [62]	CAPEX (EUR/kW)	200
	OPEX (EUR/kW)	4
	$C_{rpl}$ (EUR/kW)	150
	LF (years)	15
Hydrogen tank [51]	CAPEX (EUR/kg)	1182
	OPEX (EUR/kg)	13.6
	$C_{rpl}$ (EUR/kg)	1092
	LF (years)	20
Electrolyzer [51]	CAPEX (EUR/kW)	606
	OPEX (EUR/kW)	1.8
	$C_{rpl}$ (EUR/kW)	455
	LF (years)	5
Fuel cell [51]	CAPEX (EUR/kW)	910
	$C_{rpl}$ (EUR/kW)	774
	OPEX (EUR/kW)	0.02
	LF (years)	5

## 4. Results and Discussion

### 4.1. Economic, Environmental and Reliability Analysis

The monthly LOLP is shown in Figure 3, for each configuration. Each demand—domestic water, irrigation water, and household consumption—is indicated in the legend by the letter's "d", "ir", and "h", respectively. The fulfillment of domestic water demands

is always higher than the other two demands, as domestic water is a priority in every configuration.

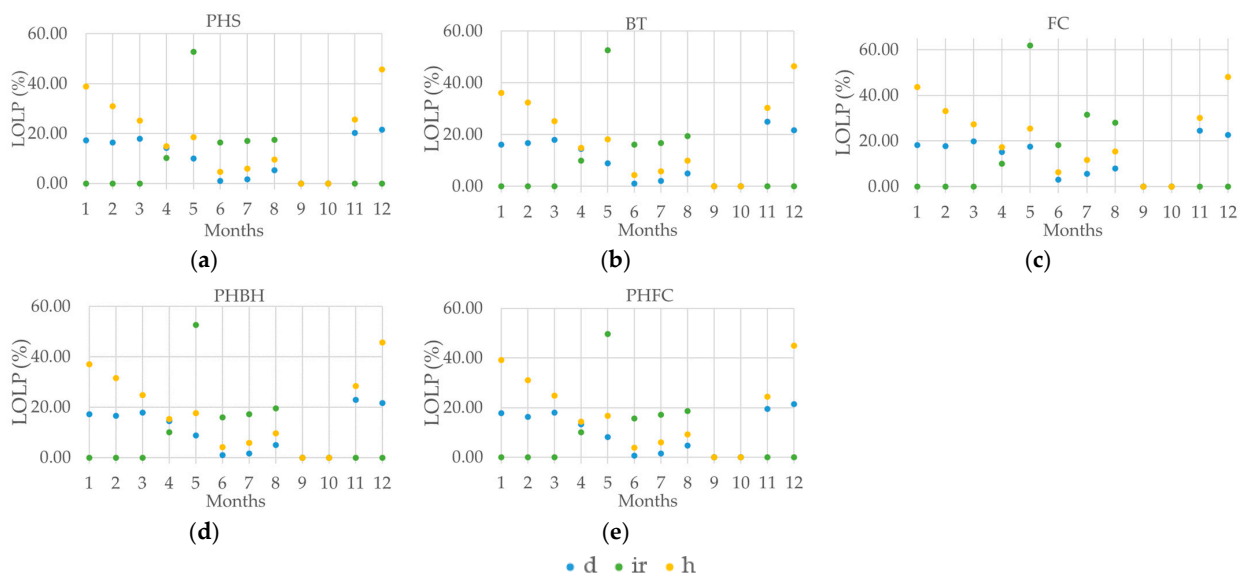


**Figure 3.** Monthly loss of load probability of different demands, d, ir and h: (a) PHS; (b) BT; (c) FC; (d) PHBH; (e) PHFC.

PHS, Figure 3a, and BT, Figure 3b, configurations show the same ‘behavior’; however, in PHS, a better fulfillment of the domestic water demand is achieved during November, compared to BT. The FC configuration, Figure 3c, shows higher results in LOLP for all three demands. This may be explained by the fact that the production of hydrogen requires significant amounts of desalinated water, and the energy of the desalination is deprived by the fulfillment of the island’s demands. Among the hybrid storage configurations, PHBH, Figure 3d, and PHFC, Figure 3e, the latter seems to result in lower values of LOLP, achieving better coverage of the demands.

In Table 6, the average LOLP for a full year (12 months) is presented for each demand—d, ir, h—and for the whole operation of the HRES—row TOTAL. Among the single-storage technologies, PHS shows better results and FC shows the minimum fulfillment of each demand. However, the configuration with the minimum use of conventional fuels is HPFC, which means that initially hybrid storage surpasses the final results and that the use of hydrogen as a second storage technology, compared to batteries, results in a reduced use of fossil fuels. This is impressive, even though the comparison of the two single-storage configurations, BT and FC, shows that BT results in lower values of LOLP for each demand examined. Also, the use of fossil fuels, and higher values of LOLP, are similar in both simple battery storage and hybrid battery storage, so the comparison should be made below with the final prices for water and energy..

**Table 6.** Loss of load probability of different demands and of the HRES based on the examined configuration.

Configuration	PHS	BT	FC	PHBH	PHFC
d	8.47	8.61	10.93	8.50	8.11
ir	21.81	21.95	29.95	22.32	21.47
h	23.08	23.25	26.51	23.02	22.66
TOTAL	21.77	21.90	25.57	21.81	21.40

Although priority is given to domestic water desalination and this demand is fulfilled by the direct penetration of RES before the storage of excess energy, the results of the

monthly amounts of domestic water that are satisfied are better in the configurations with hybrid storage technology, such as PHBH and PHFC. Among the single-storage technologies, PHS results in higher fulfillment of domestic water. Up to 87% of the monthly domestic water demand is satisfied, but as irrigation water is the least important demand in the hierarchy of significance, this percentage declines for this demand. In all of the configurations, there is full coverage autonomy for October, while the autonomy extends for the domestic water supply to June and almost to July for PHS, BT, PHBT, and PHFC. Only the FC scenario shows losses of load during both June and July in the domestic water supply.

Figure 4 displays the many energy sources that contribute each year to the island's energy mix. The share of WTs and PVs remains the same in all configurations, which is to be expected given that the choice of storage technology has little to no impact on the availability of RES in an HRES, while having a big impact on the overall participation of the storage unit. The configuration with the minimum use of fossil fuels is PHFC, which means initially that hybrid storage surpasses the results and that the use of hydrogen as a second storage unit, compared to batteries, results in reduced use of conventional fuels. Fluctuations are observed in the contribution of pumped hydro storage, battery, and hydrogen storage systems. Although all three storage systems have been sized based on their two-day autonomy, PHS and BT satisfy approximately 21% of the total demand, while FC contributes only about 17%. This indicates that the FC has less participation in the energy balance and increases the reliance on conventional fuels. Subsequently, among the configurations with simple storage, pumped storage gives better results about the use of fossil fuels, while the maximum use is observed in the single storage with a hydrogen system. In FC, this energy consumption for water desalination becomes apparent, depriving it of the fulfillment of the island's energy needs, whether it is energy needs for domestic and irrigation water desalination or energy needs for household consumption.

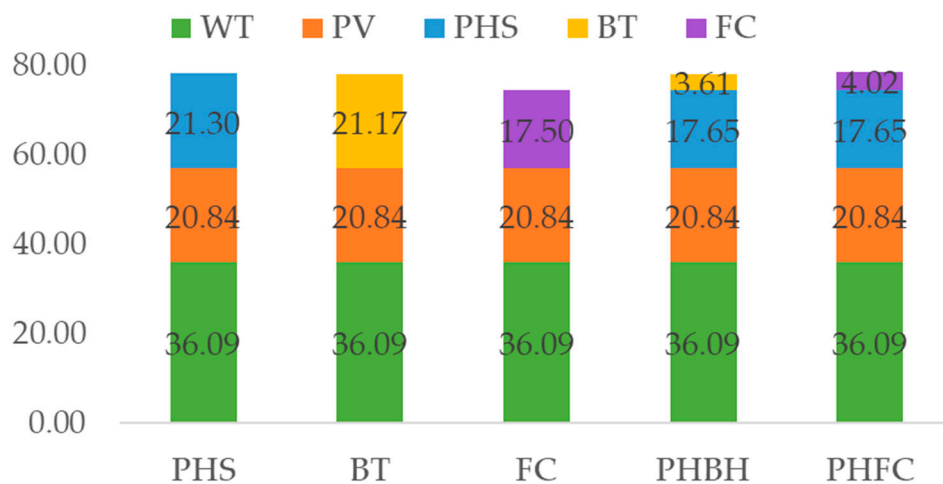


**Figure 4.** Penetration of different energy sources of HRES.

This study examines HRES coupled to various storage systems, including PHS, a battery, a hydrogen tank, or a combination of them. The energy used to desalinate water in order to meet the domestic and agricultural needs is included in the HRESs under examination. The energy consumed in the pump station for handling seawater between lower and higher reservoirs is another factor in HRESs with a PHS storage system. These hourly consumptions are depicted in Figure 5a,d,e over the period of a year (legend pumping station). The hydro turbine's hourly energy output is displayed concurrently (legend hydro turbine). Additionally, after pumping, there is energy that is not used, either because the pumps are unable to utilize it or as a result of a full reservoir that cannot store the additional water. The batteries (legend charging battery) in the PHBH and the

electrolyzer (legend electrolyzer) in the PHFC receive this unexploited energy and use it in the PHBH to charge the batteries and also use it in the PHFC to produce hydrogen. This energy is also used for the energy that is required to desalinate seawater, so that it can be utilized for electrolysis in the PHFC. In configurations (d) and (e) with the hybrid storage, the lines “charging battery” and “electrolyzer” show the energy used by the batteries and electrolyzer, respectively, and also represent the energy that cannot be utilized in the single-storage HRESs (configurations PHS, BT and FC). In the case of an energy deficit, the lines “DIScharging battery” and “fuel cell” represent the energy generated by the batteries and fuel cells, respectively. “charging battery”, “DIScharging battery”, “electrolyzer” and “fuel cell” in Figure 5b,c have similar modes of operation, with the only difference being that the excess energy from the WTs and the PVs is sent to the batteries and the electrolyzer after the initial coverage of the demands.

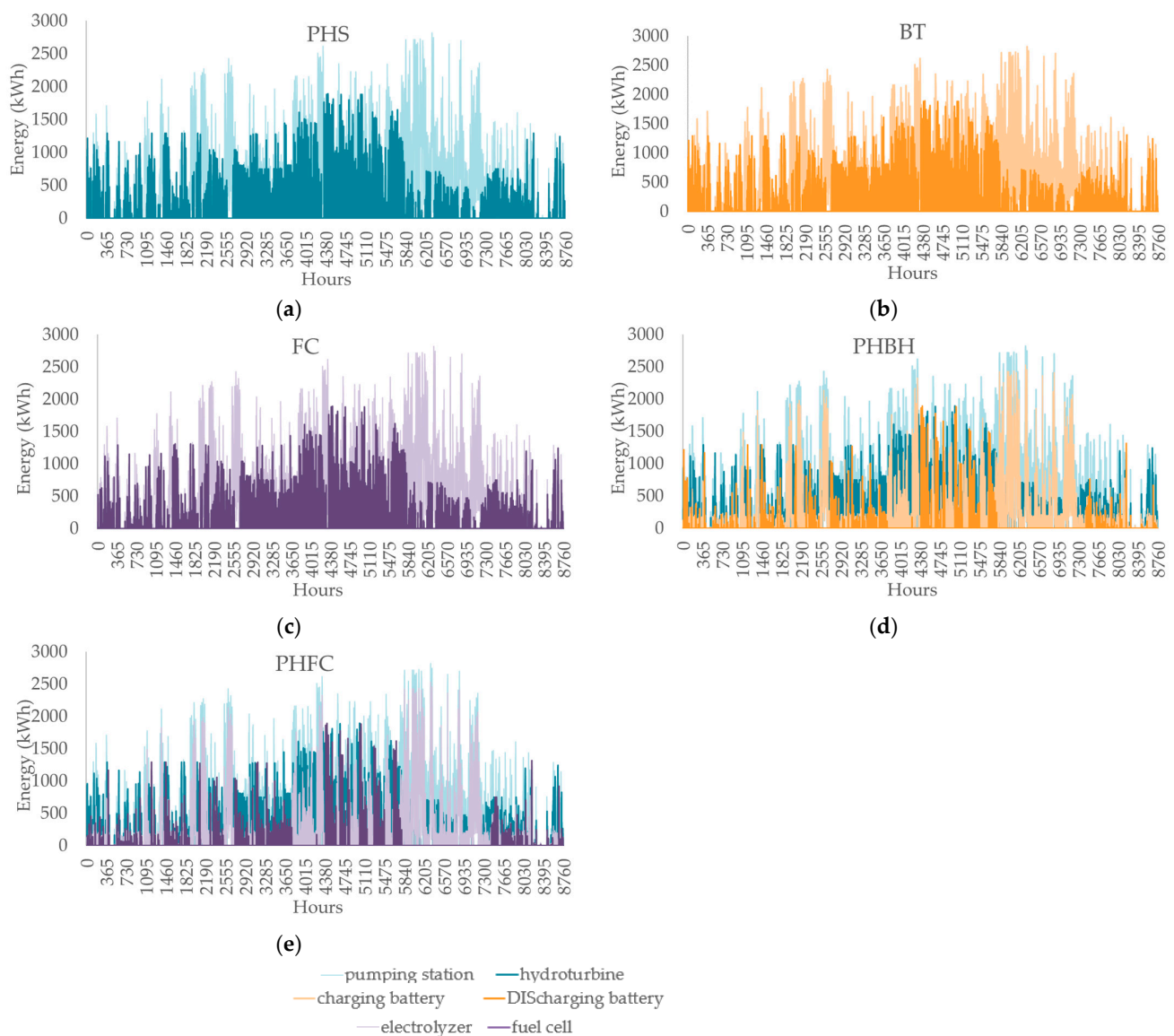


**Figure 5.** Energy distribution: (a) PHS; (b) BT; (c) FC; (d) PHBH; (e) PHFC.

The energy generated by the three different storage technologies, PHS, BT, and FC, follows a similar pattern in the systems’ attempt to fulfill the energy requirements, as illustrated in Figure 5a–c. Additionally, it is demonstrated that the energy generated by the PHS, BT, and FC systems is typically lower than the energy needed to operate the pumps, charge the batteries, and operate the electrolyzer to produce hydrogen. Even so,

the idea behind an HRES is the storage of generated RES energy that cannot be utilized at the time of production and its use at periods with high demand where the startup of the local stations, and subsequently, the consumption of fossil fuels, is the alternative solution. The different behavior of PHS, BT, and FC storage technologies, as shown in Figure 4, can be explained by considering that the energy needed by the electrolyzer for hydrogen production also includes the required energy needed for desalination. For FC storage configuration, LPS's contribution is increased throughout the year. The energy used to pump and charge the batteries seems to be more than the energy consumed during desalination in FC. However, in the comparison between the two configurations with hybrid storage, a greater contribution of FC compared to BT is observed; therefore, there is a reduced use of LPS in the case of hydrogen compared to batteries. A possible explanation is that in hybrid storage there is less and less frequent use of the secondary storage technology, FC or BT, so the time the battery is idle leads to more energy loss due to battery discharge, depending on the self-discharge rate,  $\sigma$ , of the battery.

The results about the CAPEX, the OPEX, the final price of energy and water, the LOLP, the payback period, the eliminated CO<sub>2</sub> quantities, and CO<sub>2</sub> price are presented in Table 7 for single- and hybrid-storage technologies. As COE is only influenced by CAPEX, OPEX,  $C_{slv}$ , and the energy generated by the HRES, future increases in the price of energy have no impact on COE. However, a future increase in energy will also increase the competitiveness of such attempts by decreasing the price gap. Comparisons between single-storage technologies show that PHS configurations have a lower CAPEX; however, OPEX is reduced in the case of hydrogen storage. The comparison also depends on the LOLP of each HRES. Also, the highest initial cost is seen in the case of the battery storage system. All of the above are factored into the final COE and COW values. The lowest value is observed in the PHS, followed by the FC, and finally the BT configuration. Consequently, the same sequence is followed for PBP. However, the lowest LOLP values are observed in PHS, and the maximum are observed in FC, concluding that in simple storage the PHS configuration is overall superior. Comparisons between hybrid-storage technologies show lower initial costs in PHBH, but lower maintenance costs in PHFC. Finally, concerning COE and COW, the lowest values are achieved when batteries are combined with PHS. However, as the choice must be made in conjunction with the LOLP values, lower LOLP values but also a shorter PBP are observed in the hybrid configuration consisting of PHS and hydrogen storage technology. In terms of CO<sub>2</sub> quantities and the penalty from the Emissions Trading System, PHFC presents better results. Between simple and hybrid storage, lower LOLP values are given by the hybrid storage; however, energy and water prices are comparatively higher than in the single-storage options.

**Table 7.** Economic, environmental, and reliability analysis.

Configuration	PHS	BT	FC	PHBH	PHFC
CAPEX (EUR × 10 <sup>6</sup> )	16.7	24.9	22.5	23.0	28.4
OPEX (EUR × 10 <sup>3</sup> )	514	508	299	526	423
COE (EUR/kWh)	0.215	0.281	0.241	0.267	0.292
COE (EUR/m <sup>3</sup> )	1.257	1.643	1.408	1.561	1.705
LOLP (%)	21.77	21.90	25.57	21.81	21.40
PBP (years)	11.18	14.26	12.05	13.77	10.87
$EM_{CO_2}$ (tn/year)	2286	2283	2175	2285	2297
Penalty (EUR × 10 <sup>3</sup> )	203.3	203.0	193.5	203.2	204.3

#### 4.2. Sensitivity Analysis Based on Installation, Meteorological, and Population Data

A sensitivity analysis is conducted between two single-storage configurations, PHS and FC and the hybrid PHFC, based on certain key parameters. These three configurations are compared to demonstrate how each is impacted by each important parameter. The installed height of the WTs, climate data, including wind and solar potential, and the island's inhabitants are referred to as key criteria. To demonstrate the relationship between

a variation in the value of each key parameter and the four energy, economic, and environmental indices that are estimated, COE, PBP, LOLP, and use of the storage technology (PHS and FC), each parameter is examined regarding a 10% increase and decrease. The graphic findings are shown in Figure 6.

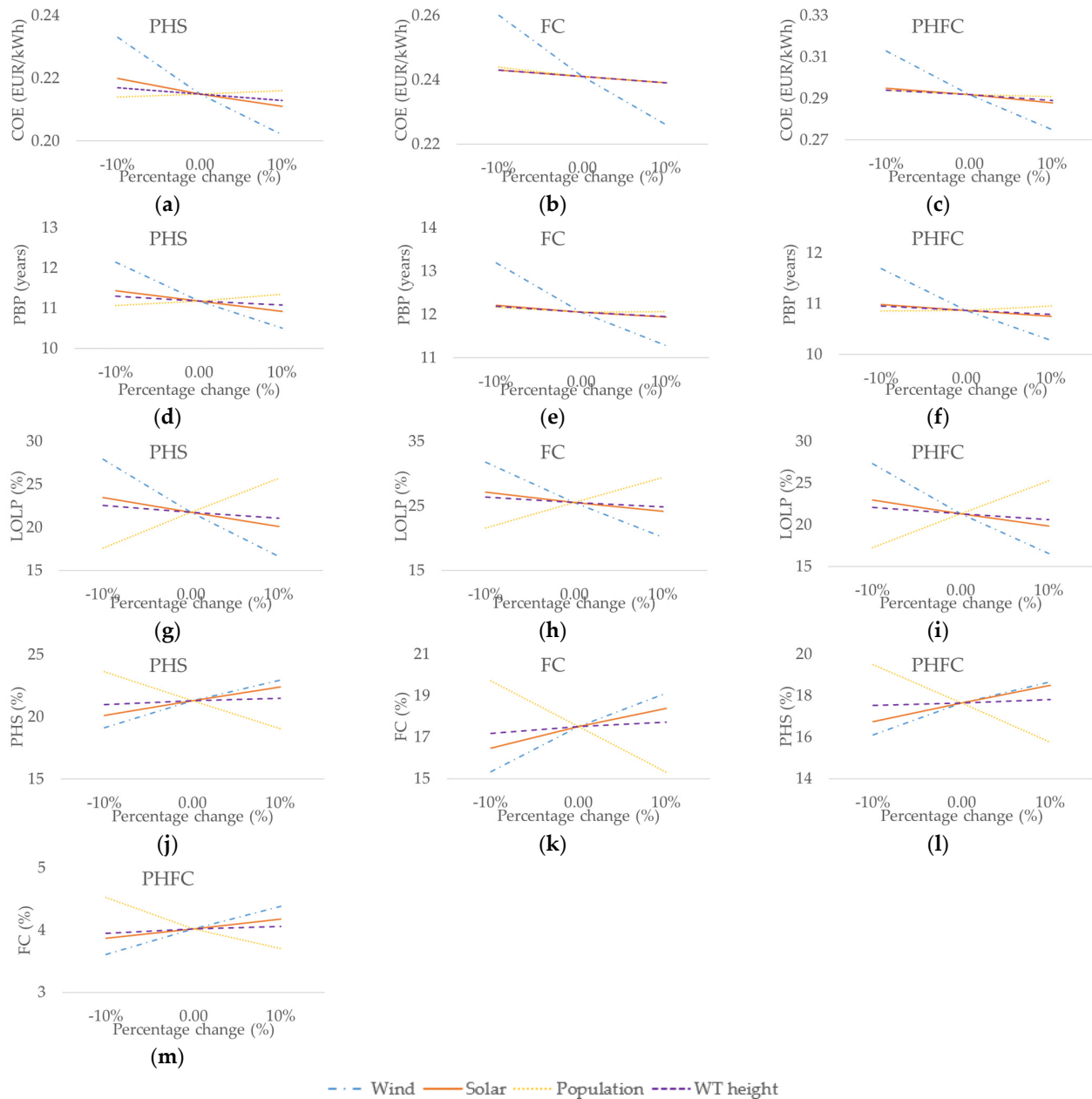


**Figure 6.** Sensitivity analysis results: for COE: (a) conf. PHS; (b) conf. FC; (c) conf. PHFC, for PBP: (d) conf. PHS; (e) conf. FC; (f) conf. PHFC, for LOLP: (g) conf. PHS; (h) conf. FC; (i) conf. PHFC, for storage unit: (j) conf. PHS; (k) conf. FC; (l) conf. PHFC-PHS unit; (m) conf. PHFC-FC unit.

The comparison between single-storage technologies, PHS and FC, shows that for both configurations, COE (Figure 6a,b), and subsequently COW, as these indices are proportional, are more impacted by modifications in the wind potential. The dependence of COE on annual RES output explains this. WTs have a bigger percentage in energy output than PVs, while having less installed capacity than PVs, probably due to the island’s greater wind potential. Additionally, compared to its decrease, the wind potential’s increase has a less significant impact. This could be due to the fact that increased wind potential cannot

always be translated into increased energy production. When the wind speed exceeds the  $u_{\text{cut-out}}$  of a WT, the WT shuts down for security reasons. In addition, compared to PHS, COE is affected more significantly by population variation in FC configuration. It is noteworthy that the demographic variance in the FC has a greater impact on COE. This may be connected to how long each system has been autonomous. As PHS provides more autonomy days, any population variance will have a greater influence on the FC system, which does not exhibit the same level of autonomy reliability. However, the population affects the PBP more (Figure 6d,e) in WT/PV/DU/PHS. Changes in population mean changes in demand, in the dimensioning of the upper reservoir, the hydro turbine, and the desalination unit, and finally, changes in CAPEX and OPEX. Also, in PHS, the LPS is operating less than in FC, where enough energy is consumed when the water needed for the electrolysis is desalinated. The same is depicted for the LOLP diagrams (Figure 6g,h), which are affected more in the FC. This is expected since the same behavior is observed in the storage unit between the two configurations. It is also remarkable that the slope of the wind potential and the population is steeper for the contribution of the FC in the FC configuration than for the contribution of the PHS in the PHS configuration (Figure 6j,k). This may be explained by the fact that, due to their capacity, the pumping station may not be able to deal with all of the extra energy, unlike FC, where variation in the wind potential and the population is better handled by the capacity of the hydrogen tank. The wind potential, the population, the solar potential, and the height of the installed WTs are classified in that order for both scenarios and all of the examined criteria. While the results are proportionate to the changes in wind and solar potential in both scenarios, they are inversely correlated to the population. Demand rises as the population grows; therefore, a bigger initial amount of RES is meant to cover both energy and water demand before the surplus is sent to the storage units.

The comparison of PHS and PHFC, which utilize single and hybrid storage, respectively, demonstrates how the WT's installation height impacts the produced amount of renewable energy produced. The cost of both electricity (see Figure 6c) and water decreases as a result of the higher installation height of the WTs. Furthermore, LOLP (Figure 6i) declines as more demands are anticipated to be supplied with increased wind energy production. The same logic applies to PBP, which falls off as WT installation height increases. COE and COW are proportionate to both models; although, regarding LOLP, changes in WT height have a greater impact on PHFC. Given that there is a second storage unit—hydrogen—this is probably expected. The potential increase in produced energy during the night due to the higher altitude of the WTs' installation also leads to the fulfillment of more irrigation water because all of the demand for irrigation water is focused during the night and simultaneously the remaining demands are minimized. The intensity of this is increased, especially if there is a backup hydrogen storage unit. Additionally, without a backup storage system from which uncovered energy may be obtained, the potential reduction in the total amount of wind energy during the night will lead to a smaller percentage of fulfillment of the irrigation demand, resulting in a more intense increase in the total LOLP. Moreover, the comparison between PHS and PHFC (Figure 6j,l,m) shows that the PHS has a different behavior than FC for changes in wind potential. Although the behavior of PHS is proportional to both increases and decreases in wind potential, the behavior of FC fluctuates. An increase in wind potential leads to a less intense increase in the FC contribution. This possibly happens as an increase in wind potential implies an increase in produced RES and therefore more demands are covered. This means that a smaller amount of energy is sent to storage, so the second storage unit is used less. Such behavior is not observed by the changes in the solar potential, possibly because better wind speeds prevail on the island throughout the year compared to solar radiation. Also, variations in population, and therefore the electrical and water demands, lead to a different behavior of COE between simple and hybrid storage systems. Population changes are proportional to COE for PHS; however, in PHFC, changes in population are inversely proportional to COE values. The COE's dependence on both HRES energy production and OPEX may

help to explain this pattern. Due to the HRES's ability to store more RES, hybrid storage systems may have higher OPEX; however, they produce more energy. Therefore, a better price is achieved for energy and desalinated water by the increase in demand. Finally, population variations lead to more intense changes in PBP (Figure 6f) and LOLP in the case of single compared to hybrid storage. Nevertheless, the comparison between FC and PHFC shows that changes of LOLP are more intense in the PHFC configuration. This indicates that changes in installation criteria, meteorological data, and demand data must always be considered when making the final decision regarding the storage technology, in addition to the initial criteria about COE or LOLP.

## 5. Conclusions

The comparison between each storage technology shows that PHS and BT generally exhibit the same "behavior"; however, PHS has lower energy and water costs, 0.215 EUR/kWh and 1.257 EUR/m<sup>3</sup>, as a result of its lower initial cost, at 16.7 million EUR. This may result in considerably cheaper pricing for energy and desalinated water, especially considering that the upper reservoir may already be constructed on the island. In this case, the initial cost is more reduced. Moreover, FC has an increased LOLP index equal to 25.57%, as desalinating the water before it enters the electrolyzer to create hydrogen requires a significant amount of energy. In all configurations, there is complete coverage autonomy for October; however, for PHS, BT, PHBH, and PHFC, the autonomy extends to June and July for the domestic water supply. Only the FC scenario exhibits load losses in the domestic water supply during July. The comparison of PHBH and PHFC reveals a greater contribution from FC in the case of hydrogen compared to batteries, as well as a lower utilization of LPS. Also, higher water and energy costs are a result of the hybrid storage arrangements, with PHFC being the greatest cost, 0.292 EUR/kWh and 1.705 EUR/m<sup>3</sup>. However, the decision must be taken in conjunction with the LOLP values, and it must be noted that PHFC exhibits lower LOLP at 21.40% and also a shorter PBP of less than 11 years. PHFC exhibits, also, better outcomes in terms of CO<sub>2</sub> amounts, 2297 tn/year, and the Emissions Trading System penalty of 204.3 thousand EUR.

According to the sensitivity analysis, FC operation is more sensitive to population fluctuations, while the COE in FC configuration is more sensitive to variations in wind potential. The population, followed by the wind potential, the solar potential, and finally, the height of the WT installation, determine the classification for both configurations and the four criteria. In the case of single storage compared to hybrid storage, population changes result in more significant changes in PBP and LOLP. Finally, a comparison of FC and PHFC reveals that the LOLP changes are more pronounced in the second configuration. This observation leads to the conclusion that the final choice of storage technology depends not only on changes in installation criteria, meteorological data, and demand data but also on changes in the initial COE, COW, or LOLP criteria.

**Author Contributions:** Conceptualization, M.M.B. and E.B.; methodology, M.M.B.; software, M.M.B.; validation, E.B.; formal analysis, M.M.B.; investigation, M.M.B.; data curation, M.M.B.; writing—original draft preparation, M.M.B.; writing—review and editing, M.M.B. and E.B.; visualization, M.M.B.; supervision, E.B. All authors have read and agreed to the published version of the manuscript.

**Funding:** This research received no external funding.

**Institutional Review Board Statement:** Not applicable.

**Informed Consent Statement:** Not applicable.

**Data Availability Statement:** Data that support the findings of this study are not publicly available due to restrictions applied to them but are available from the authors upon reasonable request and with the permission of the services that provided them.

**Conflicts of Interest:** The authors declare no conflicts of interest. The funders had no role in the design of the study; in the collection, analyses, or interpretation of data; in the writing of the manuscript, or in the decision to publish the results.

## References

1. Brini, R. Renewable and non-renewable electricity consumption, economic growth and climate change: Evidence from a panel of selected African countries. *Energy* **2021**, *223*, 120064. [CrossRef]
2. European Environment Agency. Trends and Projections in Europe 2021. Available online: <https://www.eea.europa.eu/highlights/eu-achieves-20-20-20> (accessed on 7 March 2023).
3. Paris Agreement. FCCC/CP/2015/L.9/Rev.1. UNFCCC Secretariat. Available online: <https://unfccc.int/process-and-meetings/the-paris-agreement/the-paris-agreement> (accessed on 14 November 2019).
4. He, Y.; Li, X.; Huang, P.; Wang, J. Exploring the Road toward Environmental Sustainability: Natural Resources, Renewable Energy Consumption, Economic Growth, and Greenhouse Gas Emissions. *Sustainability* **2022**, *14*, 1579. [CrossRef]
5. Sacchi, R.; Bauer, C.; Cox, B.; Mutel, C. When, where and how can the electrification of passenger cars reduce greenhouse gas emissions? *Renew. Sustain. Energy Rev.* **2022**, *162*, 112475. [CrossRef]
6. Olabi, A.; Abdelkareem, M.A. Renewable energy and climate change. *Renew. Sustain. Energy Rev.* **2022**, *158*, 112111. [CrossRef]
7. Ainou, F.Z.; Ali, M.; Sadiq, M. Green energy security assessment in Morocco: Green finance as a step toward sustainable energy transition. *Environ. Sci. Pollut. Res.* **2022**, *30*, 61411–61429. [CrossRef]
8. Cergibozan, R. Renewable energy sources as a solution for energy security risk: Empirical evidence from OECD countries. *Renew. Energy* **2022**, *183*, 617–626. [CrossRef]
9. Nasir, M.H.; Wen, J.; Nassani, A.A.; Haffar, M.; Igharo, A.E.; Musibau, H.O.; Waqas, M. Energy Security and Energy Poverty in Emerging Economies: A Step towards Sustainable Energy Efficiency. *Front. Energy Res.* **2022**, *10*, 834614. [CrossRef]
10. Liu, H.; Khan, I.; Zakari, A.; Alharthi, M. Roles of trilemma in the world energy sector and transition towards sustainable energy: A study of economic growth and the environment. *Energy Policy* **2022**, *170*, 113238. [CrossRef]
11. Al-Shetwi, A.Q. Sustainable development of renewable energy integrated power sector: Trends, environmental impacts, and recent challenges. *Sci. Total. Environ.* **2022**, *822*, 153645. [CrossRef]
12. González, D.M.L.; Rendon, J.G. Opportunities and challenges of mainstreaming distributed energy resources towards the transition to more efficient and resilient energy markets. *Renew. Sustain. Energy Rev.* **2022**, *157*, 112018. [CrossRef]
13. Janota, L.; Surovezhko, A.; Ighissenov, A. Comprehensive evaluation of the planned development of intermittent renewable sources within the EU. *Energy Rep.* **2022**, *8*, 214–220. [CrossRef]
14. Bertsiou, M.; Feloni, E.; Karpouzou, D.; Baltas, E. Water management and electricity output of a Hybrid Renewable Energy System (HRES) in Fournoi Island in Aegean Sea. *Renew. Energy* **2018**, *118*, 790–798. [CrossRef]
15. Sánchez, A.; Zhang, Q.; Martín, M.; Vega, P. Towards a new renewable power system using energy storage: An economic and social analysis. *Energy Convers. Manag.* **2022**, *252*, 115056. [CrossRef]
16. Bertsiou, M.M.; Baltas, E. Management of energy and water resources by minimizing the rejected renewable energy. *Sustain. Energy Technol. Assess.* **2022**, *52*, 102002. [CrossRef]
17. Krupnik, S.; Wagner, A.; Koretskaya, O.; Rudek, T.J.; Wade, R.; Mišák, M.; Akerboom, S.; Foulds, C.; Stegen, K.S.; Adem, Ç.; et al. Beyond technology: A research agenda for social sciences and humanities research on renewable energy in Europe. *Energy Res. Soc. Sci.* **2022**, *89*, 102536. [CrossRef]
18. Leonhardt, R.; Noble, B.; Poelzer, G.; Fitzpatrick, P.; Belcher, K.; Holdmann, G. Advancing local energy transitions: A global review of government instruments supporting community energy. *Energy Res. Soc. Sci.* **2022**, *83*, 102350. [CrossRef]
19. Dong, C.; Ji, D.; Mustafa, F.; Khursheed, A. Impacts of COVID-19 pandemic on renewable energy production in China: Transmission mechanism and policy implications. *Econ. Res. Ekon. Istraživanja* **2022**, *35*, 3857–3870. [CrossRef]
20. Zakeri, B.; Paulavets, K.; Barreto-Gomez, L.; Echeverri, L.G.; Pachauri, S.; Boza-Kiss, B.; Zimm, C.; Rogelj, J.; Creutzig, F.; Ürgé-Vorsatz, D.; et al. Pandemic, War, and Global Energy Transitions. *Energies* **2022**, *15*, 6114. [CrossRef]
21. Kushawaha, J.; Borra, S.; Kushawaha, A.K.; Singh, G.; Singh, P. Climate change and its impact on natural resources. In *Water Conservation in the Era of Global Climate Change*; Elsevier: Amsterdam, The Netherlands, 2021; pp. 333–346. [CrossRef]
22. Anderson, R.; Bayer, P.E.; Edwards, D. Climate change and the need for agricultural adaptation. *Curr. Opin. Plant Biol.* **2020**, *56*, 197–202. [CrossRef]
23. David, L.O.; Nwulu, N.I.; Aigbavboa, C.O.; Adepoju, O.O. Integrating fourth industrial revolution (4IR) technologies into the water, energy & food nexus for sustainable security: A bibliometric analysis. *J. Clean. Prod.* **2022**, *363*, 132522. [CrossRef]
24. Mamassis, N.; Efstratiadis, A.; Dimitriadis, P.; Iliopoulou, T.; Ioannidis, R.; Koutsoyiannis, D. Water and Energy. In *Handbook of Water Resources Management: Discourses, Concepts and Examples*; Springer International Publishing: Cham, Switzerland, 2021; pp. 619–657. [CrossRef]
25. Nouri, N.; Balali, F.; Nasiri, A.; Seifoddini, H.; Otieno, W. Water withdrawal and consumption reduction for electrical energy generation systems. *Appl. Energy* **2019**, *248*, 196–206. [CrossRef]
26. Myronidis, D.; Nikolaos, T. Changes in climatic patterns and tourism and their concomitant effect on drinking water transfers into the region of South Aegean, Greece. *Stoch. Environ. Res. Risk Assess.* **2021**, *35*, 1725–1739. [CrossRef]
27. Bertsiou, M.M.; Baltas, E. Power to Hydrogen and Power to Water Using Wind Energy. *Wind* **2022**, *2*, 305–324. [CrossRef]

28. Qi, X.; Wang, J.; Królczyk, G.; Gardoni, P.; Li, Z. Sustainability analysis of a hybrid renewable power system with battery storage for islands application. *J. Energy Storage* **2022**, *50*, 104682. [[CrossRef](#)]
29. Mulumba, A.N.; Farzaneh, H. Techno-economic analysis and dynamic power simulation of a hybrid solar-wind-battery-flywheel system for off-grid power supply in remote areas in Kenya. *Energy Convers. Manag. X* **2023**, *18*, 100381. [[CrossRef](#)]
30. Islam, R.; Akter, H.; Howlader, H.O.R.; Senjyu, T. Optimal Sizing and Techno-Economic Analysis of Grid-Independent Hybrid Energy System for Sustained Rural Electrification in Developing Countries: A Case Study in Bangladesh. *Energies* **2022**, *15*, 6381. [[CrossRef](#)]
31. Javed, M.S.; Ma, T.; Jurasz, J.; Mikulik, J. A hybrid method for scenario-based techno-economic-environmental analysis of off-grid renewable energy systems. *Renew. Sustain. Energy Rev.* **2021**, *139*, 110725. [[CrossRef](#)]
32. Ceylan, C.; Devrim, Y. Green hydrogen based off-grid and on-grid hybrid energy systems. *Int. J. Hydrog. Energy* **2023**, *48*, 39084–39096. [[CrossRef](#)]
33. He, Y.; Guo, S.; Zhou, J.; Wu, F.; Huang, J.; Pei, H. The quantitative techno-economic comparisons and multi-objective capacity optimization of wind-photovoltaic hybrid power system considering different energy storage technologies. *Energy Convers. Manag.* **2021**, *229*, 113779. [[CrossRef](#)]
34. Borge-Diez, D.; García-Moya, F.J.; Cabrera-Santana, P.; Rosales-Asensio, E. Feasibility analysis of wind and solar powered desalination plants: An application to islands. *Sci. Total. Environ.* **2021**, *764*, 142878. [[CrossRef](#)] [[PubMed](#)]
35. Das, P.; Das, B.K.; Rahman, M.; Hassan, R. Evaluating the prospect of utilizing excess energy and creating employments from a hybrid energy system meeting electricity and freshwater demands using multi-objective evolutionary algorithms. *Energy* **2022**, *238*, 121860. [[CrossRef](#)]
36. Bertsiou, M.; Feloni, E.; Baltas, E. Cost-benefit analysis for a Hybrid renewable energy system in Fournoi island. In Proceedings of the Sixth International Conference on Environmental Management, Engineering, Planning and Economics (CEMEPE 2017) and SECOTOX Conference, Thessaloniki, Greece, 25–30 June 2017; pp. 705–975.
37. Kiehadrouinezhad, M.; Merabet, A.; Hosseinzadeh-Bandbafha, H.; Ghenai, C. Environmental assessment of optimized renewable energy-based microgrids integrated desalination plant: Considering human health, ecosystem quality, climate change, and resources. *Environ. Sci. Pollut. Res.* **2022**, *30*, 29888–29908. [[CrossRef](#)] [[PubMed](#)]
38. Bertsiou, M.M.; Baltas, E. Energy, Economic and Environmental Analysis of a Hybrid Power Plant for Electrification, and Drinking and Irrigation Water Supply. *Environ. Process.* **2022**, *9*, 1–28. [[CrossRef](#)]
39. Blaney, H.F.; Criddle, W.D. *Determining Consumptive Use and Irrigation Water Requirements (No. 1275)*; US Department of Agriculture: Washington, DC, USA, 1962.
40. Fornarelli, R.; Shahnia, F.; Anda, M.; Bahri, P.A.; Ho, G. Selecting an economically suitable and sustainable solution for a renewable energy-powered water desalination system: A rural Australian case study. *Desalination* **2018**, *435*, 128–139. [[CrossRef](#)]
41. Xu, D.; Acker, T.; Zhang, X. Size optimization of a hybrid PV/wind/diesel/battery power system for reverse osmosis desalination. *J. Water Reuse Desalination* **2019**, *9*, 405–422. [[CrossRef](#)]
42. Psiloglou, B.; Giannakopoulos, C.; Majithia, S.; Petrakis, M. Factors affecting electricity demand in Athens, Greece and London, UK: A comparative assessment. *Energy* **2009**, *34*, 1855–1863. [[CrossRef](#)]
43. Lagouvardos, K.; Kotroni, V.; Bezes, A.; Koletsis, I.; Kopania, T.; Lykoudis, S.; Mazarakis, N.; Papagiannaki, K.; Vougioukas, S. The automatic weather stations NOANN network of the National Observatory of Athens: Operation and database. *Geosci. Data J.* **2017**, *4*, 4–16. [[CrossRef](#)]
44. Van Sark, W.G.; Van der Velde, H.C.; Coelingh, J.P.; Bierbooms, W.A. Do we really need rotor equivalent wind speed? *Wind Energy* **2019**, *22*, 745–763. [[CrossRef](#)]
45. Lin, S.; Ma, T.; Javed, M.S. Prefeasibility study of a distributed photovoltaic system with pumped hydro storage for residential buildings. *Energy Convers. Manag.* **2020**, *222*, 113199. [[CrossRef](#)]
46. Li, F.-F.; Qiu, J. Multi-objective optimization for integrated hydro-photovoltaic power system. *Appl. Energy* **2016**, *167*, 377–384. [[CrossRef](#)]
47. Cotfas, D.T.; Cotfas, P.A. Multiconcept Methods to Enhance Photovoltaic System Efficiency. *Int. J. Photoenergy* **2019**, *2019*, 1–14. [[CrossRef](#)]
48. Karami, N.; Moubayed, N.; Outbib, R. General review and classification of different MPPT Techniques. *Renew. Sustain. Energy Rev.* **2017**, *68*, 1–18. [[CrossRef](#)]
49. Notton, G.; Lazarov, V.; Stoyanov, L. Optimal sizing of a grid-connected PV system for various PV module technologies and inclinations, inverter efficiency characteristics and locations. *Renew. Energy* **2010**, *35*, 541–554. [[CrossRef](#)]
50. Simão, M.; Ramos, H.M. Hybrid Pumped Hydro Storage Energy Solutions towards Wind and PV Integration: Improvement on Flexibility, Reliability and Energy Costs. *Water* **2020**, *12*, 2457. [[CrossRef](#)]
51. Abdelshafy, A.M.; Hassan, H.; Jurasz, J. Optimal design of a grid-connected desalination plant powered by renewable energy resources using a hybrid PSO-GWO approach. *Energy Convers. Manag.* **2018**, *173*, 331–347. [[CrossRef](#)]
52. Kaldellis, J.; Kavadias, K.; Christinakis, E. Evaluation of the wind-hydro energy solution for remote islands. *Energy Convers. Manag.* **2001**, *42*, 1105–1120. [[CrossRef](#)]
53. Katsivelakis, M.; Bargiotas, D.; Daskalopulu, A.; Panapakidis, I.P.; Tsoukalas, L. Techno-Economic Analysis of a Stand-Alone Hybrid System: Application in Donoussa Island, Greece. *Energies* **2021**, *14*, 1868. [[CrossRef](#)]

54. Ceran, B.; Mielcarek, A.; Hassan, Q.; Teneta, J.; Jaszczur, M. Aging effects on modelling and operation of a photovoltaic system with hydrogen storage. *Appl. Energy* **2021**, *297*, 117161. [[CrossRef](#)]
55. Bhandari, B.; Lee, K.-T.; Lee, G.-Y.; Cho, Y.-M.; Ahn, S.-H. Optimization of hybrid renewable energy power systems: A review. *Int. J. Precis. Eng. Manuf. Technol.* **2015**, *2*, 99–112. [[CrossRef](#)]
56. Ma, T.; Javed, M.S. Integrated sizing of hybrid PV-wind-battery system for remote island considering the saturation of each renewable energy resource. *Energy Convers. Manag.* **2019**, *182*, 178–190. [[CrossRef](#)]
57. Bardis, G.; Feloni, E.; Baltas, E. Simulation and Evaluation of a Hybrid Renewable Energy System for Supplying a Desalination Unit on the Island of Lipsi, Greece. *Adv. Sci. Eng.* **2020**, *12*, 1–12. [[CrossRef](#)]
58. El-Houari, H.; Allouhi, A.; Salameh, T.; Kousksou, T.; Jamil, A.; El Amrani, B. Energy, Economic, Environment (3E) analysis of WT-PV-Battery autonomous hybrid power plants in climatically varying regions. *Sustain. Energy Technol. Assess.* **2021**, *43*, 100961. [[CrossRef](#)]
59. Greenhouse Gas Emission Intensity of Electricity Generation by Country. Available online: <https://www.eea.europa.eu/ims/greenhouse-gas-emission-intensity-of-1> (accessed on 10 September 2023).
60. Ember, Daily Carbon Prices. Available online: <https://ember-climate.org/data/data-tools/carbon-price-viewer/> (accessed on 10 September 2023).
61. Baruah, A.; Basu, M.; Amuley, D. Modeling of an autonomous hybrid renewable energy system for electrification of a township: A case study for Sikkim, India. *Renew. Sustain. Energy Rev.* **2021**, *135*, 110158. [[CrossRef](#)]
62. Jurasz, J.; Ceran, B.; Orłowska, A. Component degradation in small-scale off-grid PV-battery systems operation in terms of reliability, environmental impact and economic performance. *Sustain. Energy Technol. Assess.* **2020**, *38*, 100647. [[CrossRef](#)]

**Disclaimer/Publisher’s Note:** The statements, opinions and data contained in all publications are solely those of the individual author(s) and contributor(s) and not of MDPI and/or the editor(s). MDPI and/or the editor(s) disclaim responsibility for any injury to people or property resulting from any ideas, methods, instructions or products referred to in the content.